Quarterly Journal of the Royal Meteorological Society *Q. J. R. Meteorol. Soc.* 00: 1–19 (0000)

Moist convection and its upscale effects in the Indian Monsoon

P. D. Willetts[1*], J. H. Marsham[12], C. .E. Birch[13], D. J. Parker[1], S. Webster[4], J. Petch[4]
[1] *School of Earth and Environment, The University of Leeds, Leeds, LS2 9JT, UK.*
[2] *National Centre for Atmospheric Science, School of Earth and Environment, University of Leeds, Leeds, LS2 9JT, UK.*
[3] *MetOffice@Leeds, The University of Leeds, Leeds, LS2 9JT, UK.*
[4] *Met Office, Fitzroy Road, Exeter, EX1 3PB, UK*

*Correspondence to: School of Earth and Environment, The University of Leeds, Leeds. LS2 9JT, UK.

In common with many global models, the Met Office Unified Model (MetUM) climate simulations show large errors in Indian summer monsoon rainfall, with a wet bias over the equatorial Indian Ocean, a dry bias over India, and with too weak low-level flow into India. Here we use the first multi-day continental-scale MetUM simulations over India, with grid-spacings that allow explicit convection, to examine how convective parametrisation contributes to model biases.

Biases in the convection-permitting simulations are not always smaller than those of the parametrised simulations, but the rainfall differences over India, and reduced rainfall in the Indian Ocean enhance the monsoon circulation and transport of moisture into India, which in turn can support more rainfall there. The improved diurnal cycle of convection in convection-permitting simulations delays rainfall over land, improving the diurnal cycle in land-sea pressure gradients. The delayed convection allows greater surface insolation and, along with the altered interaction of higher rainfall intensities with the models land surface scheme, this generates a drier land surface, increasing land-sea temperature contrasts, and enhancing the onshore flow. In the convection-permitting simulations, changes in atmospheric heating from greater rainfall over land are larger than from the changes in surface insolation and, by deepening the monsoon trough, again favours water vapour transport into the continent. Similarly, reduced rainfall over the equatorial Indian Ocean in convection-permitting simulations with a sufficiently fine horizontal grid-spacing of $<\sim$4km corresponds to a relative ridge, which also enhances the land-sea pressure gradient and onshore transport. Despite changing the oceanic rainfall, changes in the low-level water vapour advection into India are dominated by changes to the flow, rather than to the moisture content in the flow. The results demonstrate the need to improve the representations of convection over both land and oceans to improve simulations of the monsoon.

Key Words:

Received ...

1. Introduction

The Indian Monsoon is the largest annual reversal in synoptic patterns of wind and rainfall in the world. Its summer rains are critical, socially and economically, to the more than one billion people of the Indian subcontinent. Most of India receives more than 80% of its annual rainfall during the summer monsoon months of June through September (Venkateswarlu and Rao 2013). It is estimated that a severe drought year reduces the gross domestic product of India by 2-5%, and that this has not changed in the last 50 years (Gadgil and Gadgil 2006). In May 2002 there was no indication from any empirical or atmospheric general circulation model that all-India rainfall in June and July would be 30% below normal (19% deficit for June through September) with a similar failure in 2004, when there was a seasonal (June through September) rainfall deficit of 13% (Gadgil *et al.* 2002, 2005). Improving forecasts for the Indian summer monsoon, on all timescales, has been linked to a need for a better understanding of the role of deep convection in the tropics (Gadgil *et al.* 2003).

The two major regions of rainfall are the Western Ghats, a mountain range running parallel to the western coast of the Indian peninsula, and the Ganges-Mahanadi Basin (GB) in north-east India (figure 1). There is also a region that runs north-west from the head of the Bay of Bengal, often referred to as the monsoon zone (Sikka and Gadgil 1980) or monsoon trough region (MT in figure 1), where transient low pressure systems which form in the Bay of Bengal or northeast India generate a significant fraction of the total Indian summer monsoon rainfall (Yoon and Chen 2005). The rainfall variability in the monsoon trough is highly correlated with all-India summer monsoon rainfall (Gadgil 2003), and as such, an improved prediction of variability in this region should also project onto the larger-scale predictability.

While global climate models (GCMs) perform reasonably well on the global scale, they fail to resolve important local to regional scale processes (Karmacharya *et al.* 2015). Most typically exhibit a systematic wet bias over the equatorial Indian Ocean, and a dry bias over central India (Sperber *et al.* 2013). Higher resolution regional climate models (RCMs), which are able to represent regional forcings, feedbacks, and processes, improve the representation of rainfall in the Indian summer monsoon, particularly over regions of steep orography such as the Himalayas and Western Ghats (Rupa Kumar *et al.* 2006). However, Lucas-Picher *et al.* (2011) show significant differences in the representation of the Indian Monsoon by a number of RCMs forced with lateral boundary conditions from the 45-year European Centre for Medium-Range Weather Forecasts (ECMWF) Re-Analysis (ERA-40) for the period 1981-2000, highlighting that they fail to properly represent important feedbacks and processes, even when biases introduced by the driving model are reduced.

The representation of convection is a dominant source of error in global models, (Jung *et al.* 2010; Sherwood *et al.* 2014), and there is evidence that the errors are primarily due to physical processes that occur on a short enough timescale (within the first few days, often the first 24 hours) to affect both weather and climate models (Rodwell and Palmer 2007; Murphy *et al.* 2004)). Improvements to convective parametrisation schemes, based on weather models, should also lead to improvements in climate models. It is expected that in the next 10 years, accounting for increases in computing power, global models of weather and climate will run at grid-spacings ranging from several kilometres, to about 100 km (Holloway *et al.* 2012b). As such, it will be necessary to parametrise convection for the foreseeable future.

Convective parametrisation schemes typically produce too many light rain events, too few heavy rain events, and have a diurnal cycle of continental precipitation that peaks too early in the day (Betts and Jakob 2002; Randall *et al.* 2003; Guichard *et al.* 2004; Stephens *et al.* 2010; Dirmeyer *et al.* 2012). The intensity and frequency of precipitation influences cloud formation and associated radiative effects, aerosol effects on the radiation balance, latent heating in the atmosphere, and surface hydrological processes (Stephens *et al.* 2010). Large amounts of moisture in the lower troposphere over India during the summer mean that small perturbations can lead to cloud formation and precipitation. Ground heating of the lower atmosphere due to insolation, which increases the lower-tropospheric instability, is an important control on the diurnal cycle of summertime convection and precipitation over the subcontinent. The diurnal cycle associated with this large and well-defined solar forcing is a fundamental mode of variability in the atmosphere, and as such has been suggested to be an important test for the correctness of any model (Yang and Slingo 2001). The atmospheric tide also contributes significantly to the diurnal cycle of convection and precipitation in the tropics (Woolnough *et al.* 2004). In addition, mesoscale circulations such as land-sea breezes, katabatic-anabatic winds, or mountain valley winds can modulate the precipitation regime and produce a diurnal cycle with distinct regional variations.

Model configurations with small enough grid-spacings to allow convection to be explicitly resolved are known to give a more realistic diurnal cycle of precipitation in the tropics, with rainfall typically peaking over land in the late afternoon (Guichard *et al.* 2004; Dirmeyer *et al.* 2012), and give a better rainfall intensity distribution, but overestimate the amount (Weisman *et al.* 1997; Holloway *et al.* 2012b). For the West African monsoon, when run over large domains for many days, convection permitting simulations have been shown to be much better on the continental scale, due in part to their improved representations of triggering, organisation and the diurnal cycle of precipitaiton (Marsham *et al.* 2013; Birch *et al.* 2014).

As part of the Earth system Model Bias Reduction and assessing Abrupt Climate project (EMBRACE; a collaboration between nineteen European partners, with the goal of improving Earth System Models), we analyse a suite of Met Office Unified Model (MetUM) simulations of a 3 week period of the 2011 Indian Summer Monsoon, over a domain size large enough to capture the monsoon system. Model configurations with sufficiently high horizontal resolution to permit the explicit resolution of cloud systems and temporal and spatial domain size large enough to allow the representation of convection to affect the continental-scale circulation, are compared with observational data and parametrised convection model configurations of the same period. Biases are expected in the convection-permitting simulations, particularly as grid-spacing increases, but the similarities among them, and their differences to the parametrised convection simulations, provide a unique insight into convection and its upscale effects in the Indian Monsoon.

Section 2 describes the EMBRACE simulations and observational data sets. Section 3 presents differences in rainfall and other diagnostics between the simulations, along with their biases compared to the satellite rainfall retrievals and surface and upper air observations, and discusses the link between the rainfall differences and the larger-scale monsoon. Section 4 gives a summary of the results and discussion.

2. Method

All simulations use the UK Met Office Unified Model (MetUM) version 8.2. The fully compressible non-hydrostatic deep-atmosphere equations of motion are solved using a semi-implicit, semi-Lagrangian scheme (Davies *et al.* 2005). It uses a staggered Arakawa C-grid in the horizontal and a terrain-following hybrid-height Charney–Phillips vertical grid. There are a comprehensive set of parametrisations for processes too complex or small-scale to be physically represented, such as surface exchange (Essery *et al.* 2001), boundary layer mixing (Lock *et al.* 2000), mixed-phase cloud microphysics (Wilson and Ballard 1999), and an optional mass flux convective parametrisation scheme (Gregory and Rowntree 1990).

The EMBRACE simulations (table 1) are a suite of MetUM simulations of a 21 day period starting 18 August 2011 00:00 UTC, which was the most anomalously wet period (and so, giving the best signal-to-noise ratio) of the 2011 Indian summer monsoon. There are 2.2, 4, 8, and 12 km grid spacing simulations that treat convection explicitly, with no convective parametrisation and a 3D Smagorinsky scheme for sub-grid mixing. While grid-spacings of 8 and 12 km would normally be considered too coarse to model without a convective parametrisation, the overlap in grid-spacings allows the effects of the representation of convection to be isolated from those due to grid-spacing (as in Marsham *et al.* (2013) for the west African monsoon). Simulations with parametrised convection at grid-spacings of 8, 12, 24 (comparable with many global numerical weather prediction models), and 120 km (comparable with many climate models) use the MetUM Global Atmosphere 4.0 (Walters *et al.* 2014) configuration, with a 1-D boundary layer scheme for the sub-grid mixing. All of these simulations have a rotated-pole horizontal grid. The convection-permitting simulations are configured as per the operational MetUM variable grid-spacing NWP model configuration (UKV) (Cullen 1993), but with the differences listed in supplementary information table S1. The simulations are nested directly within the Met UM N512L70 (~24km horizontal grid-spacing) global model ('Driving', domains in figure 1), which is reinitialised every 6 hours with Met Office operational analyses. As the Driving simulation is reinitalised every 6 hours, it is considered to be the analysis for the purpose of comparison with the free-running simulations. Hourly local boundary conditions for the free-running simulations are provided by Driving, and sea surface temperatures (SSTs) are prescribed and are updated daily from OSTIA analyses (Donlon *et al.* 2012).

Three satellite rainfall retrieval products are used for comparison with the model simulations. The Tropical Rainfall Measuring Mission (TRMM) 3B42 (version 7) rainfall product (Huffman *et al.* 2007) combines precipitation estimates from multiple satellites, and is bias-corrected with rain gauge data. It has a 0.25° by 0.25° spatial grid-spacing, and is 3 hourly. The CMORPH (CPC MORPHING technique) product (Joyce *et al.* 2004; Xie *et al.* 2013), is on an 8km horizontal grid and is half-hourly. It combines precipitation estimates from existing low orbiter microwave rainfall retrieval algorithms with spatial propagation information from infrared satellite data, which is then adjusted with daily rain gauge analysis. The Global Satellite Mapping of Precipitation (GSMaP) product (Mega *et al.* 2014), has a grid-spacing of 0.1 degree and 1 hour, and uses an algorithm to combine microwave radiometer and infrared data from multiple satellites, which is then adjusted with daily rain gauge analysis. One notable difference between these products is the use of global analysis (Japan Meteorological Agency) data, which includes precipitation profiles, in the GSMAP algorithm, while TRMM and CMORPH do not use general circulation model data in their algorithms.

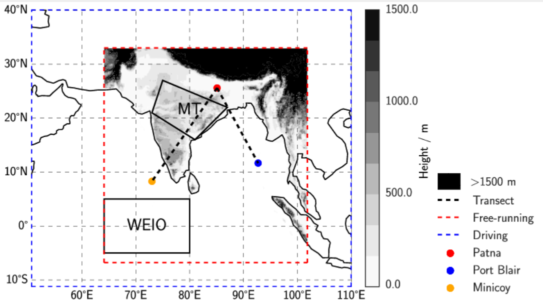

Figure 1. Simulation domains, orography, ground station locations (Patna, Port Blair and Minicoy), and regions referred to in text (Arabian Sea, Western Ghats, Monsoon Trough (MT), Bay of Bengal (BoB), Ganges-Mahanadi basin (GB), and Myanmar, and part of the Western Equatorial Indian Ocean (WEIO)). The 'subcontinent' is defined here as land west of 90°E under 3000m, BoB as ocean above 10°.

In an analysis of the performance of TRMM 3B42 and GSMAP satellite rainfall products over India, Prakash *et al.* (2015) find that while they are capable of representing large-scale spatial features and capture interannual variability, there are region-specific biases, and significant biases in rainfall amount over India (~±20%), while Xin-Xin *et al.* (2015) find good agreement in the diurnal cycle of rainfall in TRMM and CMORPH products over most of the study domain except, notably, the Tibetan Plateau. Unlike these studies, all the satellite rainfall products used in this study are adjusted with rain-gauge data, but at the time of writing, there was no quantitative assessment of their differences over the study domain. Consequently, multiple satellite rainfall products have been used to allow some understanding of the possible error in these products.

Sea level pressures measured at three surface stations (Patna, Port Blair and Minicoy in figure 1), and radiosonde sounding data from Minicoy are compared with the simulations (UK Meteorological Office 2015; Durre *et al.* 2006).

3. Results

3.1. *Rainfall*

3.1.1. *Mean pattern of rainfall*

The mean modelled distributions of rainfall are strongly affected by the representation of convection (figure 2 shows distributions for selected simulations, with plots for other model configurations, and CMORPH and GSMAP in the supporting information - figure S1). Simulations with parametrised convection give smooth distributions, while explicit convection gives much more patchy rainfall. More coarsely resolved explicit convection produces excessive rain over the ocean, which is consistent with past studies (Holloway *et al.* 2012b,a). TRMM (figure 2a) shows regions

Table 1. EMBRACE model run configurations. Domains are free-running (FR), and Driving (D) as defined in figure 1. SMAG denotes Smagorinsky scheme, Conv. is convection, 1DBL is 1-D Boundary Layer, CP is Convection Parametrised.

Grid-spacing	Domain	Timestep	Vertical Levels	Conv. Scheme	Referred to as
2.2km	FR	10s	118, 78km lid	Explicit 3D SMAG	2.2E
4km	FR	10s	118, 78km lid	Explicit 3D SMAG	4E
8km	FR	10s	118 78km lid	Explicit 3D SMAG	8E
8km	FR	300s	70, 80 km lid	1DBL + CP	8P
12km	FR	10s	118, 78km lid	Explicit 3D SMAG	12E
12km	FR	300s	70, 80 km lid	1DBL + CP	12P
24 km	FR	600s	70, 80 km lid	1DBL + CP	24P
120 km	FR	1200s	70, 80 km lid	1DBL + CP	120P
24 km	D	600s	70, 80 km lid	1DBL + CP	Driving

of higher rainfall over the Himalayas, the Myanmar coast, the Bay of Bengal, and the Western Ghats; all the simulations produce excessive rain over the orography of the Himalayas and the west coast of Myanmar, and are too dry over the Bay of Bengal and the north of the Western Ghats. Model performance in the monsoon trough region is discussed below.

The band of monsoon trough rainfall is further north in all the convection-permitting simulations, compared to TRMM (figures 2a-2c), such that there is a positive/negative dipole in the differences (figures 2e-(f)). In the parametrised simulations the band of maximum rainfall over central India is further south (figure 2d), in better agreement with TRMM, but there is deficient rainfall there and excess rainfall extending northwards to the Himalayas (figure 2d), so that the dipole of rainfall difference is due to a relatively consistent spread of rainfall over central India north of 20°N, rather than a difference in the location of the rainfall maximum. Mean total rainfall amounts in the monsoon trough, from 22 August through 6 September are between 242 and 250 mm for the three satellite rainfall retrieval products, which is relatively well captured by 2.2E, 4E, and 8E (242, 239, 237 mm respectively), although 12E rains significantly less (212 mm). The parametrised simulations rain much less in the monsoon trough, with 8P, and 12P total rainfall at 175, and 174 mm respectively. A large proportion of the rainfall in the monsoon trough comes from the propagation of a low pressure system (LPS) northwest across India from the Bay of Bengal (discussed further in section 3.2), and differences in the position of the band of monsoon trough rainfall in the free-running simulations are mostly due to the path it takes.

It is not clear from these mean spatial fields of rainfall alone that, for example, 2.2E gives a better representation than 8P of this 21 day period. The Driving simulation has the lowest rainfall biases (figure 2h) which, as it is reinitialised every 6 hours, is to be expected. The rainfall biases over the subcontinent in 2.2E may appear to be larger than those in 8P, but this is largely due to the position of the band of maximum rainfall, which in turn, is due to the path a low pressure system takes. Biases in both the convection-permitting and parametrised simulations, such as the deficient rainfall over the Bay of Bengal, can also still be useful in highlighting biases that are, to some degree, insensitive to changing grid-spacing or the representation of convection. As will be shown, the convection-permitting simulations do give a better representation of a number of aspects of the rainfall. The convection-permitting simulations also give a significantly different representation of other aspects of the monsoon system, and it is the link between convection and these differences that we aim to better understand here.

3.1.2. Temporal variability in rainfall

The total rainfall, the diurnal cycle of rainfall and rainfall intensities are all much more strongly dependent on the representation of convection than on model grid-spacing (figures 3, 4, and 5). Figure 3a shows that over the sub-continent as a whole, the convection-permitting simulations consistently rain more than the satellite retrievals and the parametrised simulations, with the exception of the

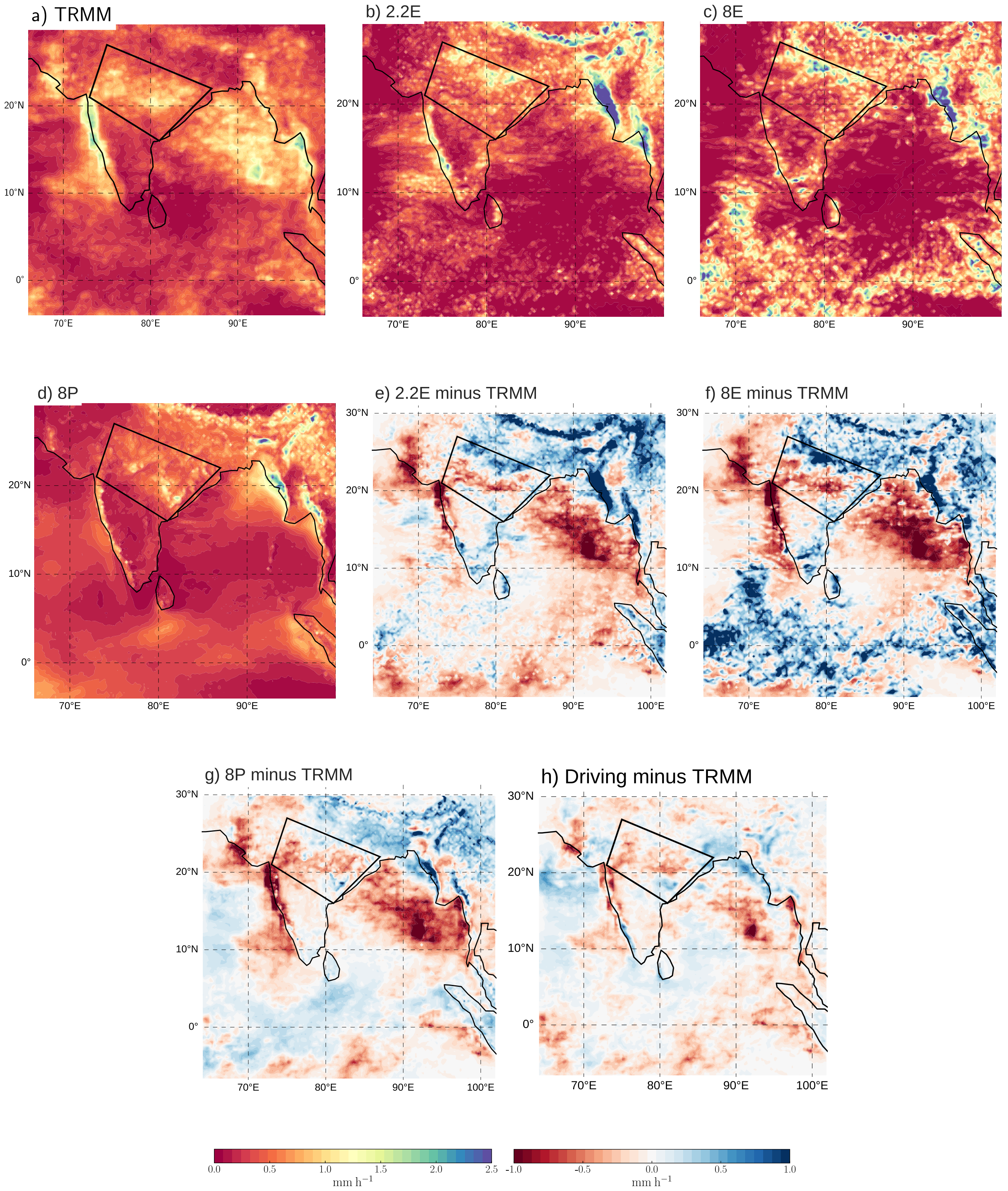

Figure 2. Mean rainfall rate and modelled rainfall rate minus TRMM (mm h^{-1}) over the 21 day period starting 18 August 2011 00:00 UTC for (a) TRMM, (b) 2.2E, (c) 8E, (d) 8P, (e) 2.2E minus TRMM , (f) 8E minus TRMM, (g) 8P minus TRMM, and (g) Driving minus TRMM. The black polygon shows the area defined as the monsoon trough. Simulations are coarse-gridded onto TRMM grid before averaging..

rainfall minimum centred around 25 August. There is a clear initial 4-day ‘spin-up’ for the convection-permitting simulations, which presumably results from the time required for convective-scale circulations to develop and the adjustment of the large-scale state of the convection-permitting simulations to their preferred atmospheric state, from that of the MetUM operational global model, which parametrises convection. Even after this spin-up, the convection-permitting simulations tend to rain more than

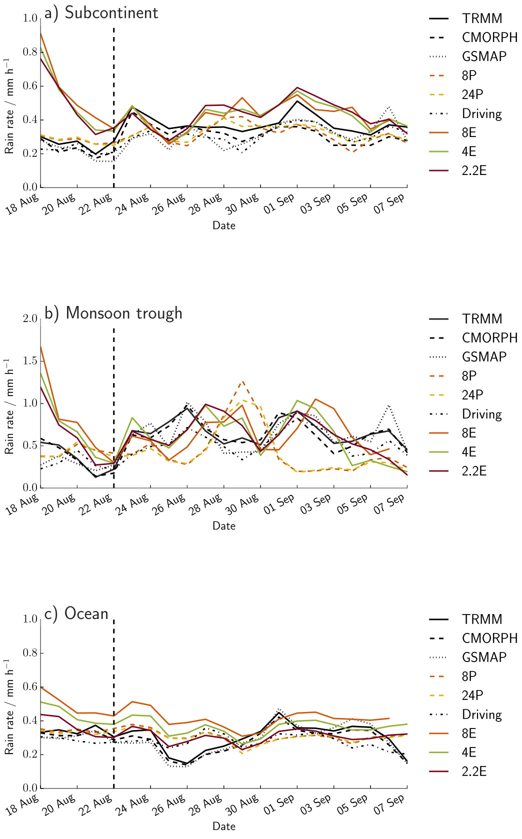

Figure 3. Daily mean rainfall rates for the 21 day simulated period over (a) the subcontinent, (b) monsoon trough, and (c) ocean, for simulations and satellite rainfall retrievals. Regions descibed or shown in figure 1). Vertical dashed line marks end of model 'spin-up' period.

Table 2. Pearson Correlation Coefficients (PCCs) between the daily mean rainfall retrievals from TRMM or CMORPH, and CMORPH, GSMAP, and a number of simulations, for the period 22 August to 7 September, after the convection-permitting simulations have spun-up. Regions descibed or shown in figure 1.

Correlated with TRMM	Subcontinent	Monsoon Trough
CMORPH	0.88	0.96
GSMAP	0.71	0.82
2.2E	0.50	0.50
4E	0.57	0.52
8E	0.46	0.05
8P	0.35	-0.27
12E	0.10	-0.26
12P	0.36	-0.26
24P	0.45	-0.27
120P	0.45	-0.20
Driving	0.68	0.83

Correlated with CMORPH	Subcontinent	Monsoon Trough
GSMAP	0.60	0.78

observed over the sub-continent figure 3a). There is a large spread in the satellite estimates of total mean rainfall over the subcontinent after spin-up, with CMORPH closer to the parametrised free-running simulations and Driving (both ~0.3 mm h^{-1}), and TRMM closer to the convection-permitting simulations ~0.37 and ~0.39 mm h^{-1}) respectively).

Among the free-running simulations, 2.2E, 4E and 8E capture the day-to-day variability over the subcontinent in TRMM the best, after the spin-up period (22 August to 7 September), with the highest Pearson Correlation Coefficients (PCC) of 0.5, 0.57, 0.46 respectively (table 2), although the PCC between TRMM and 12E is very low (0.1). Among the parametrised simulations, there is an increasing in PCC with grid-spacing in 8P, 12P, and 24P, which is similar to 120P (0.35, 0.36, 0.45, 0.46 respectively). This increase in correlation as grid spacing increases is an interesting results, but would require further investigation, which is beyond the scope of this paper. The Driving simulation, compared to TRMM, captures the day-to-day variability over the subcontinent better than the free-running simulations, with a PCC of 0.68. This is within the spread of the PCCs among the satellite rainfall retrievals (0.6 to 0.88), which is higher than the PCCs between all of the free-running simulations and TRMM.

In the monsoon trough, while the daily mean rainfall variability is much greater compared to the whole domain (figure 3b), there is still significant correlation in the day-to-day variability among the convection-permitting simulations, and among the parametrised simulations. This is particularly true after ~31 August, when the convection-permitting simulations capture the day-to-day variability in the satellite retrievals to some degree, but the rainfall drops off in the parametrised simulations and there is very little variability. Much of the variability after 31 August is associated with the propagation of a low pressure system northwest along the monsoon trough from the Bay of Bengal, and is discussed further in section 3.2). After the spin-up period, the PCCs in the monsoon trough (table 2) for 2.2E and 4E are 0.5 and 0.52 respectively, while for 8E and 12E they are both less than 0.2. These PCCs for the parametrised simulations (8P, 12P, and 24P) are all negative, between -0.2 and -0.27, while

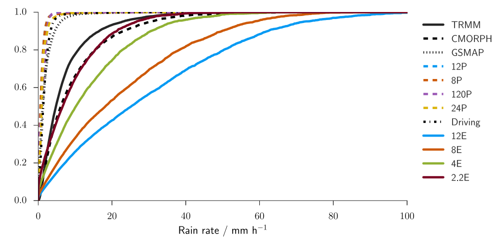

Figure 4. Cumulative sum of rainfall intensity probability distribution over the subcontinent (figure 1, between 22-30 August (figure 7)), for simulations and satellite rainfall retrievals.

the Driving simulation, as expected, has a much higher PCC at 0.83.

Figure 4 shows the cumulative sum of the fractional contribution of rainfall rates to the total rain for the simulations and satellite retrievals. A greater fraction of the total rainfall in the convection-permitting simulations and satellite observations comes from more intense rainfall, compared to the parametrised simulations, and as grid-spacing decreases, the convection-permitting distribution moves closer to that of TRMM and CMORPH. The distribution is similar among the parametrised simulations, which includes the driving simulation, with the vast majority of rain coming from light rain. There is a pronounced grid-spacing effect on the distribution among the convection-permitting simulations, with an increase in more intense rain as grid-spacing increases, although their total rainfall amounts are similar (figure 3). ~80% of the rainfall in the parametrised (free-running and driving) simulations comes from rain rates of <~3 mm h^{-1} and ~95% comes from rain rates of <~5 mm h^{-1}, while ~80% of the rainfall in the convection-permitting simulations comes from rain rates of >~3 mm h^{-1} and 60% to 20% (12E to 2.2E) comes from rain rates of >~10 mm h^{-1}. The 2.2E distribution of rainfall intensities is a close match to TRMM while the CMORPH product has a higher proportion of the rainfall coming from rain rates above ~5 mm h^{-1}. The GSMAP distribution is a close match to the parametrised simulations, and this is expected to be due to the use of model reanalysis products in its algorithm.

Consistent with past studies in other regions (Sato *et al.* 2009; Marsham *et al.* 2013), the diurnal cycle of rainfall over the subcontinent (figure 5) is much improved

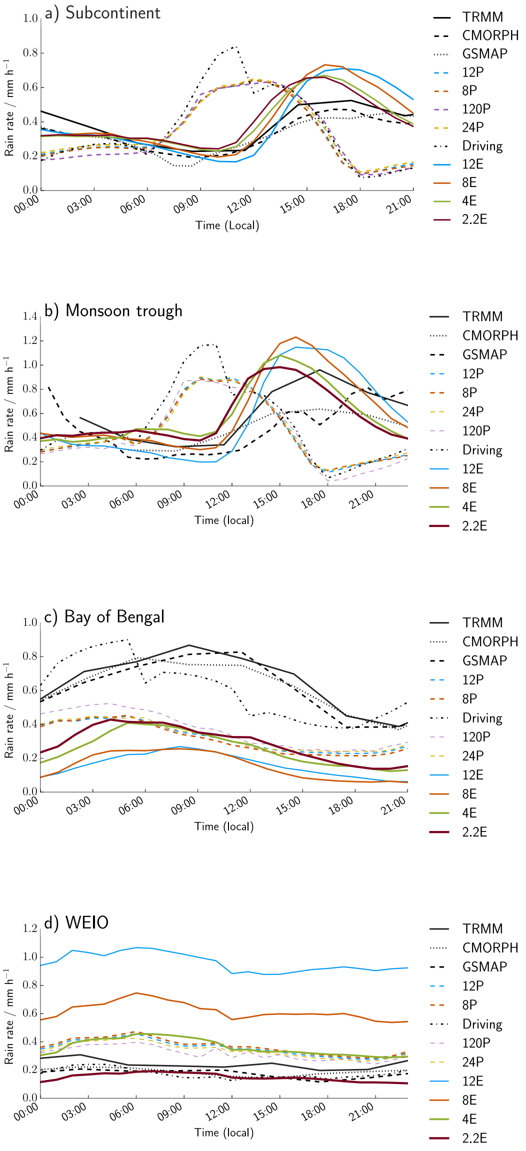

Figure 5. Mean diurnal cycle of rainfall over (a) subcontinent, (b) monsoon trough, (c) Bay of Bengal, and (d) western equatorial Indian Ocean (WEIO), for entire modelled period. Times are local times, which is UTC+5.5 hours, over central India (IST). See figure 1 for regions.

in the convection-permitting simulations, compared to the parametrised. In the convection-permitting simulations, rainfall peaks at 1500-1700 local time (India Standard Time (IST), which is UTC + 5.5 hours) and is at a minimum in the early morning, from 0800 to 1000 IST, in agreement with the satellite products, whereas rainfall in the parametrised-convection simulations peaks too early, in the morning between 0900 and 1200 IST, and is at a minimum at ~1800 IST. There is a shift among the convection-permitting simulations to a later peak in rainfall as grid-spacing increases, consistent with past studies (Petch *et al.* 2002; Marsham *et al.* 2013).

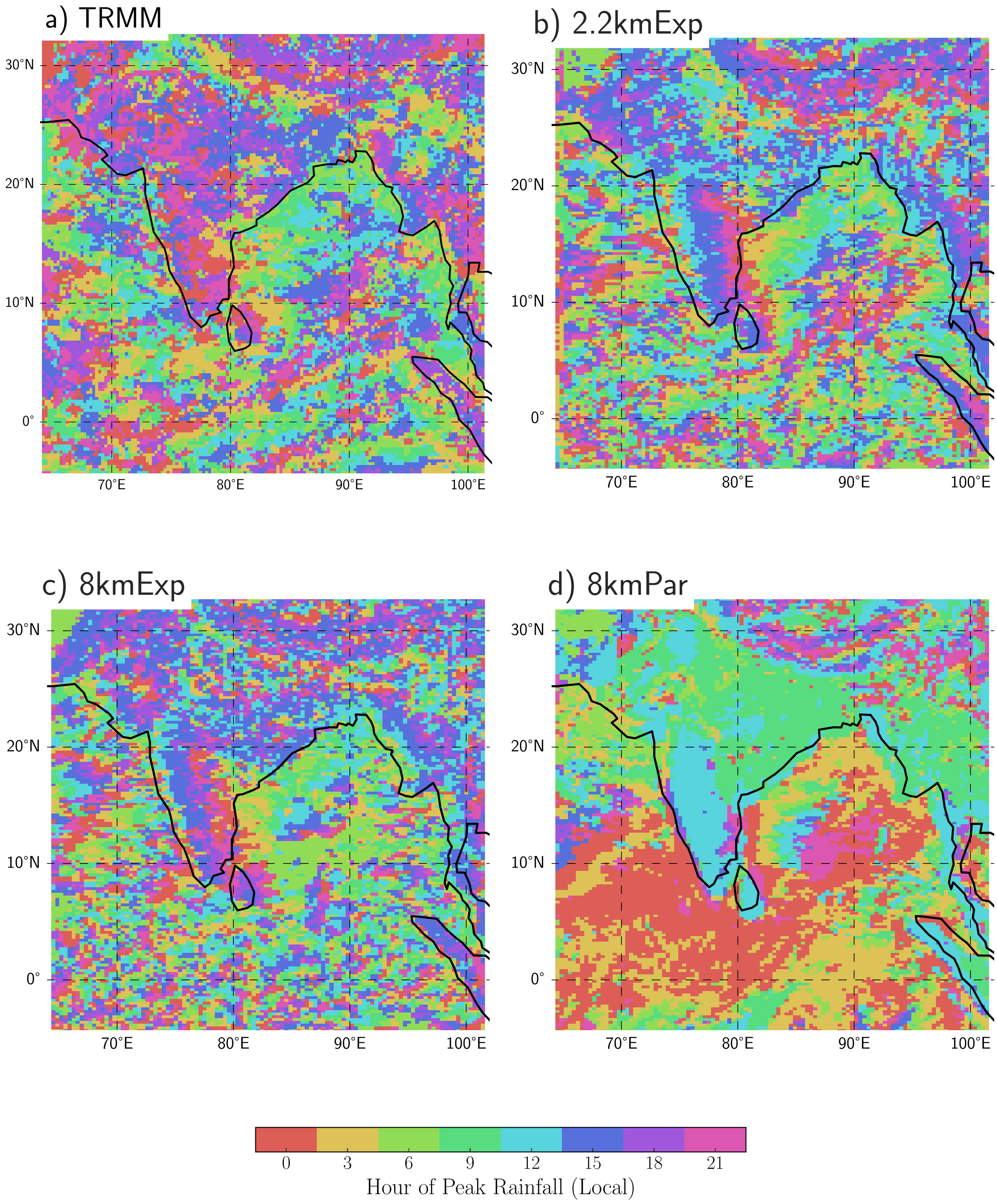

Figure 6. Mean hour of day of peak rainfall in local time (which varies with longitude, but is UTC+5.5 hours, over central India, which is IST), for EMBRACE period. Simulations coarse-grained to 24 km.

The means in figure 5 are not able to show the variety in the diurnal cycle across the land and ocean regions: this is shown in figure 6, which shows the timing of the diurnal peak in rainfall across the domain. The convection-permitting simulations capture the high degree of variability seen in TRMM, whilst the parametrised show far too little variability. TRMM and 2.2E peak rainfall timings are very similar over the oceans, with a high degree of variability which is generally not captured by the parametrised simulations. Despite this the diurnal cycle over the Bay of Bengal, with a change in peak timing in the Bay of Bengal from morning to nighttime from northwest to southeast as in TRMM, is still captured to some extent in parametrised simulations.

The time of peak rainfall in TRMM, over much of the subcontinent (particularly over the Indian peninsula, in the monsoon trough and the northwest of the domain), is 1800-0000 IST, but in 2.2E the time of peak rainfall is much more often ~1500 IST (figure 6), which is reflected in the earlier monsoon trough 2.2E mean diurnal rainfall peak, compared to the satellite observations in figure 5b. This difference is most marked over the Indian peninsula, where 2.2E rainfall in

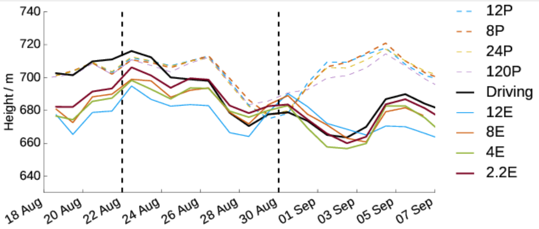

Figure 7. Daily minimum 925 hPa monsoon trough (figure 1) geopotential height (m) for simulations. The vertical dashed line on 22 August shows the end of the 'spin-up period', when the convection-permitting simulations rain far too excessively over land (figure 3). Around 30 August, the simulations diverge significantly in their representation of a low-pressure system (LPS) that propagates northwest along the monsoon trough, from the Bay of Bengal.

the lee of the Western Ghats and inshore from the east coast is between 1200-1500 IST, and 2100-0000 IST in TRMM. The 8E difference over the peninsula is less pronounced, with the night time maxima on the east coast extending further inland, and in general more of the subcontinent has later rainfall compared to 2.2E.

3.2. *Interactions between Convection and the Monsoon*

Having examined the characteristics of the modelled rainfall in section 3.1, we now use these simulations to study the interactions between the moist convection and the monsoon flow. Figure 7 shows how a change in the representation of convection produces a characteristically different monsoon trough, with a deeper trough in the convection-permitting simulations. During the first few days of spin-up, the monsoon trough is too deep in the convection-permitting simulations, but after this period they are in better agreement with Driving (i.e. analyses) than the parametrised simulations. After 31 August the parametrised and convection-permitting simulations diverge significantly. After this date, the convection-permitting simulations variability continues to correlate well with Driving, but there is a sharp increase in pressure in the parametrised simulations. This divergence is due to the propagation of a documented (Khole and Devi 2012) low pressure system, northwest from the Bay of Bengal towards Pakistan, which takes less time to move through the monsoon trough in the parametrised simulations, and accounts for the lower 925 hPa geopotential heights in the parametrised simulations during August 29-31, as well as rainfall differences in the monsoon trough (figure 3b). The remainder of our analysis therefore focuses on 22-30 August before the simulations diverge, due to differences in synoptic-scale weather, but after the spin-up of the convection-permitting simulations.

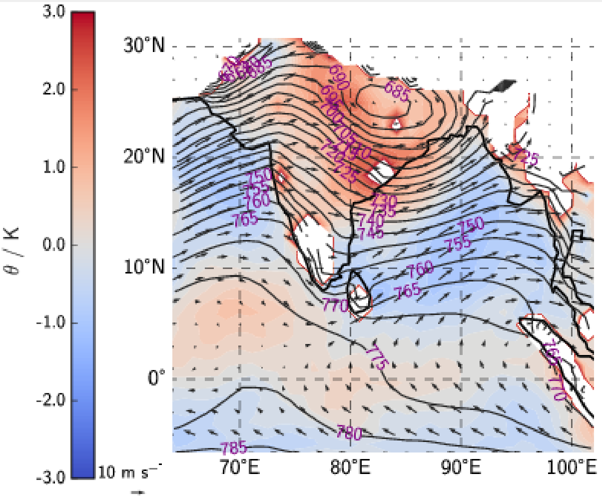

Figure 8. 8E 925 hPa geopotential height (contours), and 8E minus 8P 925 hPa potential temperature (colours), and wind vectors, between 22-30 August (figure 7). Diagnostics coarse-grained to 120km grid-spacing.

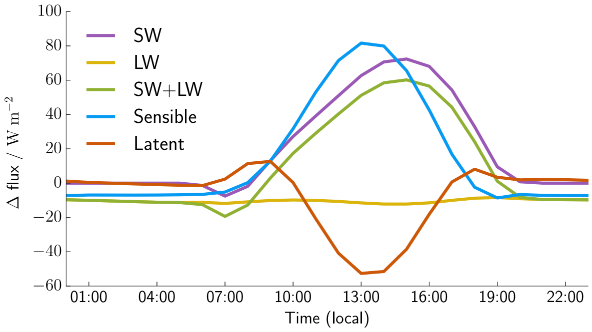

Figure 9. Diurnal cycle of 8E minus 8P surface fluxes over the subcontinent (figure 1).

Contours in figure 8 show the location of the monsoon trough as a closed low in 925 hPa height over northern India in 8E, with a gradient of increasing height to the southwest over India, and marked gradients over the the Arabian Sea and Bay of Bengal, which drive the onshore circulation of moist air into India. Colours in figure 8 show that 8E 925 hPa potential temperatures are, for the most part, 1-2 K higher over land and 1-2K lower in the Bay of Bengal and Arabian Sea, compared to 8P, which will encourage ventilation of the continent by enhancing the monsoon flow. The exception to warmer 8E temperatures over land is in the northwest of the domain (~25°N, 75°E), which is consistent with advection of cooler oceanic air driven by changes in synoptic-scale flow between the simulations (discussed below), accelerated by the boundary effect of the adjacent highlands of Pakistan,

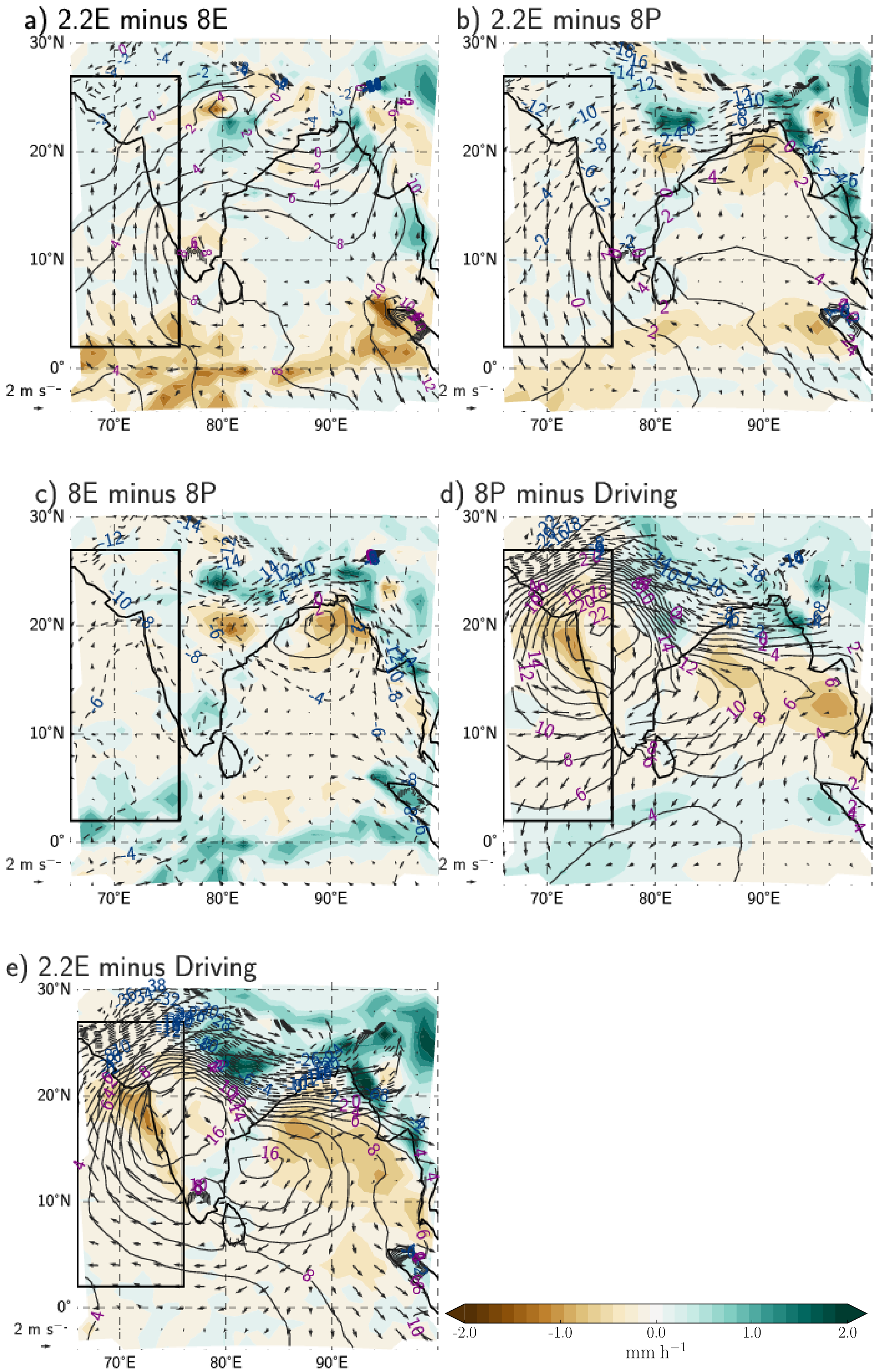

Figure 10. Simulation mean differences of 925 hPa geopotential height (contours, blue/purple contour labels for negative/positive differences), rainfall (colours), and 925 hPa wind vectors, between 22-30 August (figure 7), for (a) 2.2E minus 8E, (b) 2.2E minus 8P, (c) 8E minus 8P, (d) 8P minus Driving, and (e) 2.2E minus Driving. The black box denotes an area with significant flow differences, which is discussed in the text. Diagnostics coarse-grained to 120km grid-spacing.

into a region with no orography to impede the flow or cause the condensation of water vapour.

The greater 925 hPa temperatures over land are largely explained by the effect of the change in surface fluxes

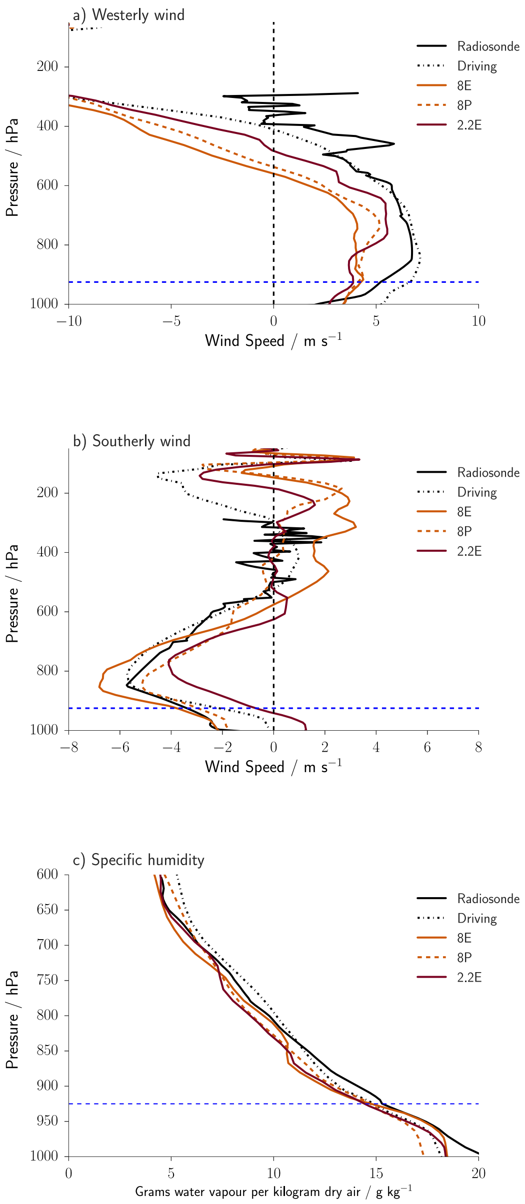

Figure 11. Mean simulated and observed vertical profiles of westerly wind, southerly wind, and specific humidity at Minicoy (figure 1), between 22-30 August (figure 7). Simulated means from times of actual soundings which at Minicoy is 9 soundings at 0100 UTC (0630 IST).

resulting from explicit convection shown in figure 9. The 925 hPa temperature differences over land, between 8E and 8P (figure 8), are attributed to the surface flux differences (figure 9) between the simulations. During the daytime, the land surface in the convection-permitting simulation receives more shortwave radiation (+20 W m^{-2} daily total mean), as a result of a later peak in clouds and convection (figure 5). Changes in net LW are smaller (-10 W m^{-2}), and so there is greater net surface heating in the convection-permitting simulation (+10 W m^{-2}). This actually gives increased sensible and reduced latent fluxes in 8E compared with 8P (+15 and -7 W m^{-2} respectively), with a Bowen ratio greater than 1 from ~1200-1500 IST in 8E, and ~0.5 throughout the day in 8P, indicating a moister surface in 8P. This can be explained by the rainfall in convection-permitting simulations being both more intense (figure 4), and later in the day (figure 5), resulting in decreased interception of rainfall by the vegetation canopy, greater run-off, and greater penetration into the soil (Best *et al.* 2011), since the rain falls after peak insolation, reducing rapid re-evaporation (Birch *et al.* 2015). 15 W m $^{-2}$ extra sensible heating in 8E, would correspond to ~0.5K extra heating for a 2km boundary layer over one day. Over the ocean, differences in 925 hPa air temperatures are smaller than over the land, since the SSTs are identical between the simulations, whereas land surface temperatures are free to evolve. Heavier rainfall in 8E over much of the western equatorial Indian Ocean (WEIO), with its greater latent heat release, is spatially correlated with the 925 hPa differences in height and potential temperature (figure 10 (a), (b)).

Rainfall differences between the free-running simulations, over both the ocean and the subcontinent, significantly alter the mean low-level pressure distribution and flow into the subcontinent (figure 10). As will be discussed, this can be seen most clearly in the region of the black box in figure 10, which covers part of the Arabian Sea and the west coast of India. The rainfall differences over land between 2.2E, 8E and 8P (figure 10 (a)- (b)), all have positive/negative dipoles in northern India, which are related to differences in the position of the monsoon trough, and although these dipoles have significant amplitude relative to their ambient amounts, they are also quite localised and have relatively little influence on the flow at larger distances, with their positive and negative anomalies cancelling each other in the far-field. For this reason, these anomalies due to the shift in location of precipitation features do not influence the continental-scale water vapour convergence budget. Where 8E rains more than 8P at ~ 24°N, 80°E, there is a relative 8E low of 16 m, whereas the relative 8P rainfall maximum at ~ 20°N, 89°E corresponds to an 8P low of 2m. In short, areas of higher rainfall in the convection-permitting simulations correspond to much larger height differences. As a result, there is a deeper monsoon trough in 2.2E and 8E compared to 8P (figure 7).

2.2E rainfall over the western equatorial Indian Ocean is the most realistic, compared to the observations (figure 5d, 10e), while 8E and 8P rain excessively (figure 10 (c), (d)). Less latent heating through rainfall over the ocean in 2.2E, compared to 8E and 8P (figure 10 (a), (b)) corresponds to a relative high, which acts to increase the pressure gradient towards the north and onshore, leading to greater southerly flow in the Arabian Sea and onto the west coast of India. 8P rains less than 8E over the WEIO (figure 10a) which will act to increase the land-sea pressure gradient in 8P, and favour an increase in the onshore flow, but 8E has a larger land-sea pressure gradient, as it is the pressure differences over the continent which are dominant in this case.

The differences in the modelled 925 hPa winds are largely consistent with a geostrophic response to these differences in geopotential over land and ocean, with an enhanced southerly cross-equatorial flow (the Somali jet), in the WEIO and Arabian Sea in 2.2E, compared to 8E and 8P, and greater onshore flow in 8E compared to 8P. Figure 11 (a), (b) shows simulated and observed (radiosonde) vertical profiles of wind at Minicoy (figure 1), which is in the Indian Ocean, in the region of the largest wind differences. 2.2E is the only simulation with southerly winds below 925 hPa, and has the weakest northerlies at the jet maximum at 850 hPa. All the free-running simulations have too weak westerlies up to ~400 hPa. It is not clear, from these simulations, what effect the domain has on the wind in the Arabian Sea. Although the enhanced southerly flow in 2.2E is actually further from the observations and analysis than 8P, the direction of the flow suggests it may be restricted by the lateral boundary conditions, and in a larger domain simulation might give an enhanced southwesterly flow, in better agreement with analyses. The increased ageostrophic wind seen on the west coast of the Indian peninsula in figure 10c (over land ~18°N, 75°E) are consistent with a response to the increased land-sea contrast discussed above. However, differences in latent heating from continental rainfall are larger than the effect on surface fluxes, and are the dominant mechanism behind the changes in the circulation. To quantify this, in the period 22-30 August, when the convection-permitting simulations have 'spun-up', and the models do not diverge due to synoptic events (figure 7), 8E rains 16mm more than 8P over the subcontinent, which corresponds to ~47 W m^{-2} atmospheric heating from rainfall, compared to ~16 W m^{-2} sensible heating from the surface.

Figure 10(a)-(c) shows differences between free-running simulations, while figure 10(d),and (e) show differences between free-running simulations and the analysis. The differences in 925 hPa winds between 2.2E/8P and Driving are relatively big, compared to the differences between, for example, 8E and 8P, with too strong southerlies coming onshore in the northwest of the domain, and too weak westerlies and southwesterlies into the southern Indian peninsula and the Bay of Bengal respectively. The free-running simulations also have a northeast to southwest dipole of excess to deficient rainfall in the monsoon trough, which match with the wind differences. Although the differences between the free-running simulations and the analysis are large, they are similarly large in 2.2E and 8P, compared to the differences between them.

The enhanced low-level monsoon circulation in 2.2E and 8E brings more moisture into the sub-continent, which supports the increased rainfall. Figure 11 (c) shows simulated and observed vertical profiles of specific humidity at Minicoy. While there are large differences in the low-level flow over Minicoy (figure 10) , the profiles of specific humidity are comparatively very similar. As such, differences in the representation of convection and grid-spacing do not, in these simulations, have a large impact on the moisture content of air advected over the Arabian Sea, and the change in the transport of moisture into the subcontinent is determined by changes in the flow, not moisture content

In previous work using numerical models, excess rainfall over the WEIO has been found to contribute to a dry bias over India, but the mechanisms by which the rainfall biases are reduced are different to those presented here. Bush *et al.* (2014) find that increasing the entrainment factor by 1.5

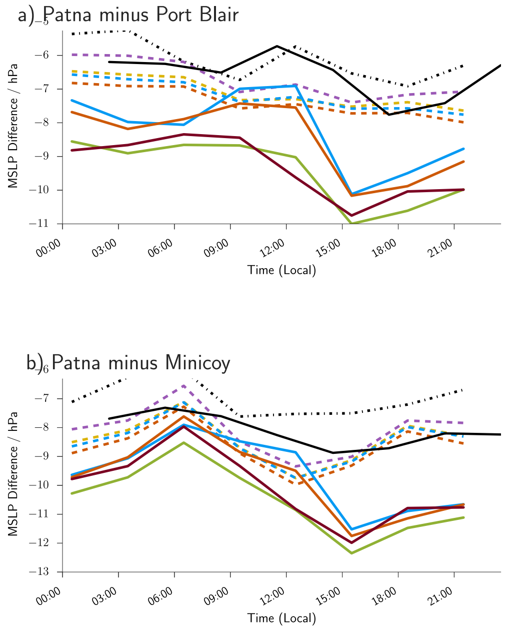

Figure 12. Diurnal cycle of mean sea-level pressure difference between (a)) central India (Patna) and Bay of Bengal (Port Blair), and (b) central India and Arabian Sea (Minicoy). See figure 1 for station locations. Observations are surface station data.

in the WEIO suppresses precipitation there which, unlike in these simulations, increases moisture in the Somali jet, and increases precipitation over the Arabian Sea and Bay of Bengal, just outside the area of increased entrainment, and over central India by a small fraction of the MetUM bias. One theory is that the meridional SST gradient in the WEIO has a large effect on the distribution of precipitation in simulations of the ISM (Bollasina and Ming 2013). The SST gradient induces low-level wind convergence, and it is the interaction of the model parametrisation schemes with this large-scale forcing that leads to excess rainfall over the WEIO. In addition to weakening the low-level monsoon flow, Bollasina and Ming (2013) find that excess rainfall over the WEIO induces a Hadley-type circulation which has a descending branch over northeast India/Indochina that, for example, leads to a more gradual onset over India.

3.2.1. Diurnal Cycle of Pressure

The change in convection not only affects the mean synoptic pattern (figure 10), but its diurnal cycle (figure 12). The simulations are compared here to surface station data, as opposed to model analyses, which are significantly affected by their representation of convection. The diurnal cycle of MSLP at any point depends on atmospheric tides, which are global-scale periodic oscillations of the atmosphere (Woolnough *et al.* 2004), and have a large amplitude in the tropics (Basu 2007). However, the effect of tides is fairly consistent across the domain and as such differences in the diurnal cycle in SLP between two points, especially those on a similar longitude, is dominated by synoptic effects. Differences in the diurnal cycle of land-sea pressure gradient between the simulations will affect the low-level onshore advection of moisture by the monsoon circulation, which will have important implications over India and the surrounding oceans.

Figure 12 shows the simulated and observed diurnal cycle of sea-level pressure (SLP) difference between the monsoon trough and Port Blair (Bay of Bengal) and Minicoy (Arabian Sea). As the sea level pressure for stations above sea level is derived from the measured surface pressure, differences in the magnitude of the pressure gradient are here considered less important than the relative mangitude and timings of the diurnal variation. In both, the largest land-sea pressure gradient is between 1500 and 1800 IST, at the time of peak rainfall over the continent, which matches well with the convection-permitting simulations, as does the smallest pressure gradient in the morning (1100 IST Port Blair gradient, 0700 IST Minicoy). The two diurnal cycles of land-sea pressure gradient differ much more in the parametrised simulations. Between the monsoon trough and Port Blair, the largest land-sea pressure gradient is around 2200 IST, and between Patna and Minicoy, it is around 1200 IST, which are too late and too early respectively. One major difference between the Patna to Port Blair transect, and the Patna to Minicoy transect, is the proportion of land to ocean along the transect, and this can explain the differences in the diurnal cycle in the parametrised simulations. There is mostly ocean between Patna and Port Blair, and the diurnal cycle of the pressure gradient in the parametrised simulations appears to be related to the diurnal cycle of rainfall in the Bay of Bengal (figure 5c), with the largest onshore pressure gradient at night, when the oceanic rainfall is at its lowest, while the more intense continental rainfall in the convection-permitting simulations (figure 4) dominates in modulating the Patna to Port Blair diurnal cycle. There is mostly land between Patna and Minicoy, and as such the diurnal cycle of pressure in the parametrised simulations is much more related to their diurnal cycle of continental rainfall (figure 5a).

The results are consistent with the late afternoon heating from moist convection in the monsoon trough region driving a decrease in the pressure over land in the convection-permitting simulations, and increasing the pressure gradient. The land-sea pressure gradient is then greatest at night, in agreement with the observations, when the drag effect of continental boundary layer covection is at a minimum. It shows that the ability of the simulations to capture the diurnal cycle of convection is not only important for radiation and surface fluxes (figure 9), but also for the dynamical couplings between convection and the larger scale flows.

4. Conclusions

Most global climate models have a systematic dry bias over India during the Indian summer monsoon, and a wet bias over the equatorial Indian Ocean. To investigate the role convective parametrisation plays in the development of these systematic model biases, convection-permitting simulations with grid spacings of 2.2, 4, 8 and 12 km, and convection-parametrised simulations with grid spacings of 8, 12, 24, and 120 km, are compared with model analyses and satellite and ground station observations. The simulations are of an anomalously wet three week period during August and September 2011, to improve the signal-to-noise ratio, with a domain that covers the subcontinent and its surrounding oceans, and captures the monsoon circulation over the subcontinent.

There is more rainfall over the subcontinent in the convection-permitting simulations, which is more intense and peaks later in the day. The 2.2E convection-permitting simulation gives the best representation of the diurnal cycle, and intensity of continental rainfall, compared to the observations. In general, there is better day-to-day variability in the amount of rainfall over the continent in the convection-permitting simulations. The convection-permitting simulations rain more, over the subcontinent, than the satellite rainfall retrievals and the parametrised simulations. In the monsoon trough, the convection-permitting simulations rain a similar amount to the satellite rainfall retrievals (which have a much lower spread than over the subcontinent), while the parametrised simulations rain much less. Satellite rainfall retrievals are known to have significant biases in the amount of rainfall over India (~20%). While the convection-permitting simulations rainfall is excessive over land, the difference between them and the parametrised simulations has been used here to examine the effects of a dry bias over India, in simulations that parametrise convection.

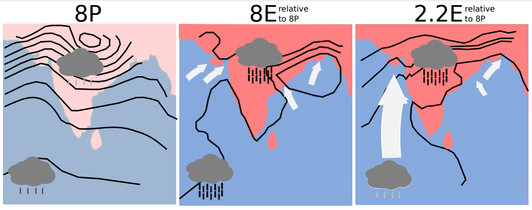

Figure 13. Schematic illustrating relative differences in rainfall (over India and the western equatorial Indian ocean) and 925 hPa height (contours), wind (arrow) and temperature, between 8P, 8E and 2.2E. The left panel shows the 8P 925 hPa mean height structure, while the middle and right panels show the respective height anomaly from 8P. Wind and rainfall are relative to 8P.

The relationship between rainfall and some other aspects of the Indian monsoon are shown schematically in figure 13. Higher rainfall, from more intense convection, increases the pressure gradient in the convection-permitting simulations and, subsequently, the onshore advection of moisture. The later convection in the convection-permitting simulations also leads to greater surface solar shortwave heating, due to reduced cloud cover during the middle of the day, and, in combination with the higher intensity of the rainfall, greater sensible heating due to a drier land surface. The greater insolation and sensible heating at the surface contributes to a larger land-sea temperature gradient, which leads to enhanced ageostrophic flow. As a result of the improved diurnal cycle of rainfall in the convection-permitting simulations over land, the diurnal cycle of the land-sea pressure gradient is improved, and the land-sea pressure gradient is enhanced in the late afternoon and at night, when the drag effect of boundary layer convection on the synoptic flow is reduced or nonexistent.

Rainfall over the equatorial Indian Ocean, through its effect on the onshore pressure gradient, is found to be an important factor in reducing low-level flow and moisture transport into the subcontinent. In the convection-permitting simulations decreasing the grid-spacing from 8km to 2.2km substantially reduces the rainfall over the Western Equatorial Indian Ocean (WEIO), in better agreement with the observations. Reduced rainfall there leads to an increase in the onshore pressure gradient, and as a result there is more southerly geostrophic flow onto the Indian peninsula, from the WEIO. However, it is difficult to say how the western boundary of the model domain affects these flow differences. It is possible that in a larger domain simulation, which includes the cross-equatorial Somali jet circulation, reduced rainfall over the WEIO would enhance that flow (which may also become moister) rather than the southerly flow shown here. The observed and simulated vertical profiles of specific humidity within these large flow differences do not differ greatly, compared to the wind differences, such that it is the strength of the monsoon circulation, and not the moisture content of the flow, that is important in reducing biases in the transport of moisture into the Indian subcontinent.

After the first 4 days of the simulation, when the convection-permitting simulations have spun-up and are adjusted to their preferred atmospheric state, they capture the time evolution of the monsoon trough depth for the remainder of the simulated period (22 August to 7 September), whereas the monsoon trough in the parametrised simulations is generally not deep enough. The propagation of a low pressure system (LPS) from the Bay of Bengal northwest along the monsoon trough, in the second half of the simulated period, causes significant divergence between the convection-permitting and parametrised simulations, as seen in the monsoon trough 925hPa height, where the convection-permitting simulations capture the daily variability in the analysis, but the height increases significantly in the parametrised simulations. The divergence appears to be related to differences in the speed of propagation of the LPS in the free-running simulations, with it taking less time to propagate northwest in the parametrised simulations. If models that parametrise convection consistently exhibit a similar bias in the propagation of LPSs, this could contribute to a systematic dry bias in parametrised convection simulations over the subcontinent, and would also have an effect on the onshore moisture transport through a weaker land-sea pressure gradient. Further work is needed to determine if there is a systematic bias in the propagation speed of LPSs over along the Indian monsoon trough, as a result of a convective parametrisation.

The convection-permitting simulations have their own biases, and in some respects perform worse than the parametrised simulations, particularly at coarser grid-spacings. All the simulations overestimate rainfall over the Himalayas and the orography of the Myanmar coastline, and underestimate rainfall over the WG. They also fail to capture the broad spread of rainfall over the Bay of Bengal. 2.2E rainfall over the Indian Ocean is comparable to TRMM, but as grid-spacing increases, rainfall in the convection-permitting simulations becomes increasingly excessive, while there is little effect due to grid-spacing in the parametrised simulations, which have rainfall amounts comparable to TRMM.

The MetUM, in common with many models has had a long standing dry bias over India during the monsoon. The results show that an explicit representation of convection affects the entire monsoon circulation, increasing rainfall in the monsoon trough region, and improving key aspects of the circulation such as the magnitude and diurnal cycle of pressure gradient from the oceans to the continent.

We conclude that it is important for any parametrisation of convection to capture its diurnal cycle, and give an improved representation of rainfall intensities over the Indian subcontinent and the western equatorial Indian Ocean, if they are to give a realistic coupling between convection and the monsoon.

Acknowledgements

We acknowledge the TRMM mission scientists and associated NASA personnel for the production of the TRMM data used in this paper and are grateful to the Goddard Earth Sciences Data and Information Services Center (GES DISC) for making the data available. The CMORPH data were obtained from NOAA CPC, from their website at ftp://ftp.cpc.ncep.noaa.gov/precip/global_CMORPH/. The GSMaP Project was sponsored by JST-CREST and is promoted by the JAXA Precipitation Measuring Mission (PMM) Science Team, and the GSMaP products were distributed by the Earth Observation Research Center, Japan Aerospace Exploration Agency. The radiosonde data were obtained from NOAA NCEI, from their website at https://www.ncdc.noaa.gov/data-access/weather-balloon/integrated-global-radiosonde-archive.

This work was funded by a Natural Environment Research Council PhD scholarship (NE/K006932/1; Met Office CASE).

References

Basu BK. 2007. Diurnal Variation in Precipitation over India during the Summer Monsoon Season: Observed and Model Predicted. *Monthly Weather Review* **135**(6): 2155–2167, doi: 10.1175/MWR3355.1.

Best MJ, Pryor M, Clark DB, Rooney GG, Essery RLH, Ménard CB, Edwards JM, Hendry MA, Porson A, Gedney N, Mercado LM, Sitch S, Blyth E, Boucher O, Cox PM, Grimmond CSB, Harding RJ. 2011. The Joint UK Land Environment Simulator (JULES), model description – Part 1: Energy and water fluxes. *Geosci. Model Dev.* **4**(3): 677–699, doi:10.5194/gmd-4-677-2011.

Betts AK, Jakob C. 2002. Evaluation of the diurnal cycle of precipitation, surface thermodynamics, and surface fluxes in the ECMWF model using LBA data. *Journal of Geophysical Research: Atmospheres* **107**(D20): LBA 12–1, doi:10.1029/2001JD000427.

Birch CE, Parker DJ, Marsham JH, Copsey D, Garcia-Carreras L. 2014. A seamless assessment of the role of convection in the water cycle of the West African Monsoon. *Journal of Geophysical Research: Atmospheres* **119**(6): 2013JD020 887, doi: 10.1002/2013JD020887. 00001.

Birch CE, Roberts MJ, Garcia-Carreras L, Ackerley D, Reeder MJ, Lock AP, Schiemann R. 2015. Sea-breeze dynamics and convection initiation: The influence of convective parameterization in weather and climate model biases. *Journal of Climate* **28**(20): 8093–8108.

Bollasina MA, Ming Y. 2013. The general circulation model precipitation bias over the southwestern equatorial Indian Ocean and its implications for simulating the South Asian monsoon. *Climate Dynamics* **40**(3-4): 823–838, doi:10.1007/s00382-012-1347-7. 00006.

Bush SJ, Turner AG, Woolnough SJ, Martin GM, Klingaman NP. 2014. The effect of increased convective entrainment on Asian monsoon biases in the MetUM General Circulation Model. *Quarterly Journal of the Royal Meteorological Society* : n/a–n/adoi:10.1002/qj.2371.

Cullen M. 1993. The Unified Forecast Climate Model. *Meteorological Magazine* **122**(1449): 81–94. WOS:A1993LG31800001.

Davies T, Cullen MJP, Malcolm AJ, Mawson MH, Staniforth A, White AA, Wood N. 2005. A new dynamical core for the Met Office's global and regional modelling of the atmosphere. *Quarterly Journal of the Royal Meteorological Society* **131**(608): 1759–1782, doi:10.1256/qj.04.101.

Dirmeyer PA, Cash BA, Iii JLK, Jung T, Marx L, Satoh M, Stan C, Tomita H, Towers P, Wedi N, Achuthavarier D, Adams JM, Altshuler EL, Huang B, Jin EK, Manganello J. 2012. Simulating the diurnal cycle of rainfall in global climate models: resolution versus parameterization. *Climate Dynamics* **39**(1-2): 399–418, doi:10.1007/s00382-011-1127-9.

Donlon CJ, Martin M, Stark J, Roberts-Jones J, Fiedler E, Wimmer W. 2012. The Operational Sea Surface Temperature and Sea Ice Analysis (OSTIA) system. *Remote Sensing of Environment* **116**: 140–158, doi:10.1016/j.rse.2010.10.017. 00094.

Durre I, Vose RS, Wuertz DB. 2006. Overview of the Integrated Global Radiosonde Archive. *Journal of Climate* **19**(1): 53–68, doi:10.1175/JCLI3594.1. 00275.

Essery R, Best M, Cox P. 2001. Moses 2.2 technical documentation. Technical report, Hadley Centre Technical Note.

Gadgil S. 2003. The Indian Monsoon and Its Variability. *Annual Review of Earth and Planetary Sciences* **31**(1): 429–467, doi: 10.1146/annurev.earth.31.100901.141251. 00229.

Gadgil S, Gadgil S. 2006. The Indian Monsoon, GDP and Agriculture. *Economic and Political Weekly* **41**(47): 4887–4895, URL http://www.jstor.org/stable/4418949. [Online; accessed 22-March-2016].

Gadgil S, Rajeevan M, Nanjundiah R. 2005. Monsoon prediction - Why yet another failure? *Current Science* **88**(9): 1389–1400.

Gadgil S, Srinivasan J, Nanjundiah RS, Kumar KK, Munot A, Kumar KR. 2002. On forecasting the indian summer monsoon: the intriguing season of 2002. *CURRENT SCIENCE-BANGALORE-* **83**(4): 394–403.

Gadgil S, Vinayachandran PN, Francis PA. 2003. Droughts of the Indian summer monsoon: Role of clouds over the Indian Ocean. *Current Science* **85**(12): 1713–1719.

Gregory D, Rowntree PR. 1990. A Mass Flux Convection Scheme with Representation of Cloud Ensemble Characteristics and Stability-Dependent Closure. *Monthly Weather Review* **118**(7): 1483–1506, doi:10.1175/1520-0493(1990)118<1483:AMFCSW>2.0.CO;2.

Guichard F, Petch J, Redelsperger JL, Bechtold P, Chaboureau JP, Cheinet S, Grabowski W, Grenier H, Jones C, Köhler M, Piriou JM, Tailleux R, Tomasini M. 2004. Modelling the diurnal cycle of deep precipitating convection over land with cloud-resolving models and single-column models. *Quarterly Journal of the Royal Meteorological Society* **130**(604): 3139–3172, doi:10.1256/qj.03.145. 00127.

Holloway CE, Woolnough SJ, Lister GMS. 2012a. The Effects of Explicit versus Parameterized Convection on the MJO in a Large-Domain High-Resolution Tropical Case Study. Part I: Characterization of Large-Scale Organization and Propagation*. *Journal of the Atmospheric Sciences* **70**(5): 1342–1369, doi:10.1175/JAS-D-12-0227.1. 00000.

Holloway CE, Woolnough SJ, Lister GMS. 2012b. Precipitation distributions for explicit versus parametrized convection in a large-domain high-resolution tropical case study. *Quarterly Journal of the Royal Meteorological Society* **138**(668): 1692–1708, doi:10.1002/qj.1903. 00014.

Huffman GJ, Bolvin DT, Nelkin EJ, Wolff DB, Adler RF, Gu G, Hong Y, Bowman KP, Stocker EF. 2007. The TRMM Multisatellite Precipitation Analysis (TMPA): Quasi-Global, Multiyear, Combined-Sensor Precipitation Estimates at Fine Scales. *Journal of Hydrometeorology* **8**(1): 38–55, doi:10.1175/JHM560.1.

Joyce RJ, Janowiak JE, Arkin PA, Xie P. 2004. CMORPH: A method that produces global precipitation estimates from passive microwave and infrared data at high spatial and temporal resolution. *Journal of Hydrometeorology* **5**(3): 487–503, doi:10.1175/1525-7541(2004)005%3C0487:CAMTPG%3E2.0.CO;2.

Jung T, Balsamo G, Bechtold P, Beljaars ACM, Köhler M, Miller MJ, Morcrette JJ, Orr A, Rodwell MJ, Tompkins AM. 2010. The ECMWF model climate: recent progress through improved physical parametrizations. *Quarterly Journal of the Royal Meteorological Society* **136**(650): 1145–1160, doi:10.1002/qj.634. 00041.

Karmacharya J, Levine RC, Jones R, Moufouma-Okia W, New M. 2015. Sensitivity of systematic biases in South Asian summer monsoon simulations to regional climate model domain size and implications for downscaled regional process studies. *Climate Dynamics* : 1–19doi:10.1007/s00382-015-2565-6.

Khole M, Devi SS. 2012. MONSOON SEASON (June to September 2011). *Mausam* **63**(3): 511–528, URL `http://metnet.imd.gov.in/mausamdocs/36331.pdf`. [Online; accessed 22-March-2016].

Lock AP, Brown AR, Bush MR, Martin GM, Smith RNB. 2000. A New Boundary Layer Mixing Scheme. Part I: Scheme Description and Single-Column Model Tests. *Monthly Weather Review* **128**(9): 3187–3199, doi:10.1175/1520-0493(2000)128<3187:ANBLMS>2.0.CO;2.

Lucas-Picher P, Christensen JH, Saeed F, Kumar P, Asharaf S, Ahrens B, Wiltshire AJ, Jacob D, Hagemann S. 2011. Can Regional Climate Models Represent the Indian Monsoon? *Journal of Hydrometeorology* **12**(5): 849–868, doi:10.1175/2011JHM1327.1.

Marsham JH, Dixon NS, Garcia-Carreras L, Lister GMS, Parker DJ, Knippertz P, Birch CE. 2013. The role of moist convection in the West African monsoon system: Insights from continental-scale convection-permitting simulations. *Geophysical Research Letters* **40**(9): 1843–1849, doi:10.1002/grl.50347.

Mega T, Ushio T, Kubota T, Kachi M, Aonashi K, Shige S. 2014. Gauge adjusted global satellite mapping of precipitation (GSMaP_gauge). In: *General Assembly and Scientific Symposium (URSI GASS), 2014 XXXIth URSI*. pp. 1–4, doi:10.1109/URSIGASS.2014.6929683.

Murphy JM, Sexton DMH, Barnett DN, Jones GS, Webb MJ, Collins M, Stainforth DA. 2004. Quantification of modelling uncertainties in a large ensemble of climate change simulations. *Nature* **430**(7001): 768–772, doi:10.1038/nature02771. 00957.

Petch JC, Brown AR, Gray MEB. 2002. The impact of horizontal resolution on the simulations of convective development over land. *Quarterly Journal of the Royal Meteorological Society* **128**(584): 2031–2044, doi:10.1256/003590002320603511.

Prakash S, Mitra AK, Rajagopal EN, Pai DS. 2015. Assessment of TRMM-based TMPA-3B42 and GSMaP precipitation products over India for the peak southwest monsoon season. *International Journal of Climatology* : n/a–n/adoi:10.1002/joc.4446.

Randall D, Khairoutdinov M, Arakawa A, Grabowski W. 2003. Breaking the Cloud Parameterization Deadlock. *Bulletin of the American Meteorological Society* **84**(11): 1547–1564, doi:10.1175/BAMS-84-11-1547. 00406.

Rodwell MJ, Palmer TN. 2007. Using numerical weather prediction to assess climate models. *Quarterly Journal of the Royal Meteorological Society* **133**(622): 129–146, doi:10.1002/qj.23.

Rupa Kumar K, Sahai AK, Krishna Kumar K, Patwardhan SK, Mishra PK, Revadekar JV, Kamala K, Pant GB. 2006. High-resolution climate change scenarios for India for the 21st century. *Current Science* **90**(3): 334–345.

Sato T, Miura H, Satoh M, Takayabu YN, Wang Y. 2009. Diurnal Cycle of Precipitation in the Tropics Simulated in a Global Cloud-Resolving Model. *Journal of Climate* **22**(18): 4809–4826, doi: 10.1175/2009JCLI2890.1.

Sherwood SC, Bony S, Dufresne JL. 2014. Spread in model climate sensitivity traced to atmospheric convective mixing. *Nature* **505**(7481): 37–42, doi:10.1038/nature12829. 00023.

Sikka DR, Gadgil S. 1980. On the maximum cloud zone and the ITCZ over Indian, longitudes during the southwest monsoon. *Monthly Weather Review* **108**(11): 1840–1853, doi:10.1175/1520-0493(1980)108%3C1840:OTMCZA%3E2.0.CO;2. 00506.

Sperber KR, Annamalai H, Kang IS, Kitoh A, Moise A, Turner A, Wang B, Zhou T. 2013. The Asian summer monsoon: an intercomparison of CMIP5 vs. CMIP3 simulations of the late 20th century. *Climate Dynamics* **41**(9-10): 2711–2744, doi:10.1007/s00382-012-1607-6.

Stephens GL, L’Ecuyer T, Forbes R, Gettlemen A, Golaz JC, Bodas-Salcedo A, Suzuki K, Gabriel P, Haynes J. 2010. Dreary state of precipitation in global models. *Journal of Geophysical Research: Atmospheres* **115**(D24): D24 211, doi:10.1029/2010JD014532.

UK Meteorological Office. 2015. Met office (2012): Met Office Integrated Data Archive System (MIDAS) Land and Marine Surface Stations Data (1853-current). NCAS British Atmospheric Data Centre.

Venkateswarlu B, Rao V. 2013. Climate change and its impact on indian agriculture. In: *Climate Change Modeling, Mitigation, and Adaptation*, pp. 419–453.

Walters DN, Williams KD, Boutle IA, Bushell AC, Edwards JM, Field PR, Lock AP, Morcrette CJ, Stratton RA, Wilkinson JM, Willett MR, Bellouin N, Bodas-Salcedo A, Brooks ME, Copsey D, Earnshaw PD, Hardiman SC, Harris CM, Levine RC, MacLachlan C, Manners JC, Martin GM, Milton SF, Palmer MD, Roberts MJ, Rodríguez JM, Tennant WJ, Vidale PL. 2014. The Met Office Unified Model Global Atmosphere 4.0 and JULES Global Land 4.0 configurations. *Geosci. Model Dev.* **7**(1): 361–386, doi: 10.5194/gmd-7-361-2014.

Weisman ML, Skamarock WC, Klemp JB. 1997. The Resolution Dependence of Explicitly Modeled Convective Systems. *Monthly Weather Review* **125**(4): 527–548, doi:10.1175/1520-0493(1997)125<0527:TRDOEM>2.0.CO;2. 00316.

Wilson DR, Ballard SP. 1999. A microphysically based precipitation scheme for the UK meteorological office unified model. *Quarterly Journal of the Royal Meteorological Society* **125**(557): 1607–1636, doi:10.1002/qj.49712555707.

Woolnough SJ, Slingo JM, Hoskins BJ. 2004. The Diurnal Cycle of Convection and Atmospheric Tides in an Aquaplanet GCM. *Journal of the Atmospheric Sciences* **61**(21): 2559–2573, doi: 10.1175/JAS3290.1.

Xie P, Joyce R, Sun F, Wu S, Yarosh Y, Yoo S. 2013. A reprocessed and bias-corrected high-resolution satellite derived precipitation record covering the entire trmm/gpm era. In: *AGU Fall Meeting Abstracts*, vol. 1. p. 03.

Xin-Xin Z, Xun-Qiang BI, Xiang-Hui K. 2015. Observed diurnal cycle of summer precipitation over South Asia and East Asia based on CMORPH and TRMM satellite data. *Atmospheric and Oceanic Science Letters* **8**(4): 201–207, doi:10.3878/AOSL20150010.

Yang GY, Slingo J. 2001. The Diurnal Cycle in the Tropics. *Monthly Weather Review* **129**(4): 784–801, doi:10.1175/1520-0493(2001)129<0784:TDCITT>2.0.CO;2. 00441.

Yoon JH, Chen TC. 2005. Water vapor budget of the Indian monsoon depression. *Tellus A* **57**(5): 770–782, doi:10.1111/j.1600-0870.2005.00145.x. 00020.